Applied Catalysis B: Environmental 84 (2008) 65–74

Contents lists available at ScienceDirect

Applied Catalysis B: Environmental

journal homepage: www.elsevier.com/locate/apcatb

Kinetic modeling of photocatalytic degradation reactions: Effect of charge trapping

Asefeh Jarandehei, Mojgan Karimi Golpayegani, Alex De Visscher *

University of Calgary, Schulich School of Engineering, Department of Chemical and Petroleum Engineering & Centre for Environmental Engineering Research and Education (CEERE), 2500 University Drive, N.W., Calgary, AB, Canada, T2N 1N4

ARTICLE INFO

Article history:
Received 12 September 2007
Received in revised form 5 March 2008
Accepted 12 March 2008
Available online 21 March 2008

Keywords:
Charge trapping
Kinetic modeling
Photocatalytic degradation
UV irradiance

ABSTRACT

This study investigates the important role of charge trapping in a photocatalytic degradation kinetic model. Different charge trapping reactions were coupled with photocatalytic degradation reaction schemes. The resulting kinetic models were applied to formate and trichloroethylene (TCE) in aqueous and gas phase, respectively. In both cases addition of charge trapping improved the reliability of the kinetic models. Hence, two dissipative charge reactions are considered in the new model: electron–hole recombination with second-order kinetics and charge trapping with first-order kinetics. For the formate system, it was shown that accounting for UV irradiance effects on a mechanistic basis requires the incorporation of charge trapping effects in the kinetic model. The improved model fitted literature data to within experimental error. A reasonable mechanism was suggested for degradation of TCE which involves three electron–hole pairs for the complete mineralization of one molecule of TCE. A kinetic model of TCE degradation via three main steps, along with considering charge trapping can explain the kinetic data with the same accuracy as an existing model of Demeestere et al., but with a more realistic electron–hole pair requirement, and added flexibility to account for light intensity effects.

1. Introduction

Photocatalysis is a promising technology which utilizes semiconductors like TiO_2, ZnO, WO_3, $FeTiO_3$, and $SrTiO_3$ to carry out a photo-induced redox process that may degrade volatile organic compounds (VOCs) into CO_2 and H_2O, and completely remove NO_x and SO_x. Particularly, this technique is promising for the degradation of VOCs, in both gaseous and aqueous phase [1]. Potential applications in the gas phase include waste gas treatment [2], indoor air pollutant abatement [3,4], and ambient air pollutant removal [5,6]. Nowadays, due to the contribution of these compounds to environmental problems such as tropospheric ozone formation, stratospheric ozone layer depletion and global warming, photocatalytic degradation of VOCs is gaining more and more interest [7].

To initiate a photocatalytic reaction, photons with sufficient energy to overcome the band gap of the semiconductor are needed. For TiO_2, with a band gap of 3.2 eV, the wavelength should be lower than approximately 390 nm. Therefore, UV light with a wavelength between 300 and 365 nm is a practical choice for photocatalysis. With sufficient energy for activation, the electrons will transfer between valence bands and conduction bands to form electron–hole pairs on the catalyst surface. Some of the electron–hole pairs take part in reactions with adsorbed molecules while some others recombine and dissipate the input energy as heat, and/or get trapped [8,9].

The energy of a photon is related to the wavelength, and overall energy input to a photocatalytic process is dependent upon the UV irradiance, the amount of light energy striking a surface per unit of time. Therefore, the effect of both UV irradiance and wavelength is important [4]. The increase of UV irradiance can increase the formation of electron–hole pairs on the TiO_2 surface which leads to increased reaction rate.

However, the increased recombination of these pairs can reduce the quantum yield [10]. Quantum yield is the number of photochemical events per absorbed photon. A related term is the quantum efficiency which is the rate of a given step depopulating a given species, divided by the sum of the rates of all steps depopulating that species [11]. For a primary photochemical process the two are the same. Because the term quantum yield is recommended for monochromatic systems only, we will use the term quantum efficiency.

The effect of UV irradiance on photocatalytic degradation of different kinds of VOCs has been investigated by some researchers. They have applied the power law to relate UV irradiance to degradation rate, where the power law index (or order) depends on

* Corresponding author. Fax: +1 403 284 4852.
E-mail address: adevissc@ucalgary.ca (A. De Visscher).

0926-3373/$ – see front matter © 2008 Elsevier B.V. All rights reserved.
doi:10.1016/j.apcatb.2008.03.006

Nomenclature

$[F]_{ads}$	concentration of formate in adsorbed phase (mmol g^{-1})
$[F]_l$	concentration of formate in liquid phase (g l^{-1})
$[h^+]$	concentration of holes (mmol g^{-1})
h_{trap}	concentration of trapped holes (mmol g^{-1})
I	photon absorption rate per gram of catalyst (meinstein g^{-1} s^{-1})
k_{ads}	intermediate product adsorption rate constant (m^3 g^{-1} s^{-1})
k_{des}	intermediate product desorption rate constant (s^{-1})
K_F	linear formate liquid–solid adsorption equilibrium constant (l g^{-1})
k_F	adsorbed formate reaction rate constant (l g^{-1})
k_p	intermediate products conversion rate constant (g $mmol^{-1}$ s^{-1})
k_{recomb}	electron–hole recombination rate constant (g $mmol^{-1}$ s^{-1})
k_{reg}	regeneration reaction rate constant (mmol g^{-1} s^{-1})
k_{TCE}	TCE conversion rate constant (g $mmol^{-1}$ s^{-1})
K_{TCE}	the linear TCE gas–solid adsorption equilibrium constant (m^3 g^{-1})
k'_{trap}	trapping reaction rate constant (g $mmol^{-1}$ s^{-1})
r_{ads}	intermediate product adsorption rate (mmol g^{-1} s^{-1})
r_{des}	intermediate product desorption rate (mmol g^{-1} s^{-1})
r_F	conversion rate of adsorbed formate (mmol g^{-1} s^{-1})
r_{light}	electron–hole production rate (mmol g^{-1} s^{-1})
r_{recomb}	electron–hole recombination rate (mmol g^{-1} s^{-1})
r_{reg}	reaction rate of regeneration (mmol^2 g^{-2} s^{-1})
r_{trap}	reaction rate of trapping reaction (mmol g^{-1} s^{-1})
T	total trap concentration (mmol g^{-1})
$[TCE]_{ads}$	adsorbed TCE concentration (mmol g^{-1})
$[TCE]_g$	gaseous TCE concentration (mmol m^3)
[trap]	free trap concentration (mmol g^{-1})
Φ_F	quantum efficiency of formate photocatalysis (–)

the efficiency of electron–hole formation and recombination at the catalyst's surface. It takes a value between 0.5 and 1 providing the reaction is kinetically controlled [12]. The value of 0.61 was suggested by Wang et al. [13] for photocatalytic degradation of trichloroethylene (TCE) in gas phase employing 365 nm UV light over titanium dioxide (TiO_2) on glass beads.

At weak intensities, the observed rate of oxidation is first-order with respect to radiation intensity, and shifts to half-order once the rate of electron–hole formation becomes greater than the photocatalytic rate, favoring electron–hole recombination [14].

It is necessary to consider electron–hole pair formation and charge trapping in kinetic models to have an adequate fit to experimental data under all conditions. This is because transition from light-unsaturated to light-saturated conditions leads to a decrease of reaction order with respect to UV irradiance. The effect of UV irradiance, charge trapping and electron–hole formation and recombination is not considered in most of the kinetic models. However, they have been taken into account in some recent works [8]. The main kinetic model that has been used in previous work is the Langmuir–Hinshelwood model [15–18].

Ma and Ku [19] investigated the reaction kinetics of the photocatalytic oxidation of gaseous TCE using TiO_2 at UV irradiance of 2.82 W/m^2. They combined the UV irradiance factor and Langmuir–Hinshelwood rate equation to develop an expression for TCE photocatalytic degradation. They obtained a reaction order of 0.52008 with respect to UV irradiance. Yamazaki et al. [20], Salvado-Estivill et al. [21], and Wang et al. [22] applied the same model for kinetics and the same approach to considering the effect of UV irradiance. Yamazaki et al. [20] examined the effect of UV irradiance on the degradation rate of ethylene over a TiO_2 photocatalyst. They showed that, for the conditions of their experiment, the reaction rate is first-order with respect to the UV irradiance. This finding indicates that the system is not performing under light saturation. Thus, higher intensities will produce higher rates without losing efficiency, i.e., at a constant quantum efficiency. Salvado-Estivill et al. [21] showed that TCE conversion rate is dependent on the UV irradiance, up to 28.1 W/m^2, with the power of one. Linear dependency of reaction rate to UV irradiance below 18.3 W/m^2, was observed by Wang et al. [22] for photodegradation of benzene over TiO_2. Also Obee and Brown [23] applied formaldehyde, toluene and 1,3-butadiene as the reactants to study the effect of UV irradiance on photocatalytic oxidation. For illumination levels far above one sun (the sun emits about 10–20 W/m^2 for wavelengths below 350 and 400 nm, respectively) equivalent, the oxidation rate increased with the square root of the UV irradiance. However when it was below one sun, the oxidation rate increased linearly with the UV irradiance. For toluene the oxidation rate dependency on UV irradiance in the range of 10–40 m W/m^2, followed a power law with an exponent of 0.55. The authors reached the same conclusion for formaldehyde and 1,3-butadiene.

A new kinetic model, explicitly taking into account electron–hole pair reactions, was developed by Demeestere et al. [7] based on linear TCE adsorption–desorption equilibrium and first order reaction kinetics. The model accounts for competition between TCE degradation, the degradation of reaction products, and electron–hole pair recombination. It was shown that the model gives a more adequate fit to experimental data than Langmuir–Hinshelwood kinetics. However, the number of predicted intermediate reaction steps involving electron–hole pairs by this model is too large to be interpreted by a reasonable mechanism, and the effect of charge trapping was neglected. Also, the UV irradiance dependency of the model was not tested. As the radiation field was homogeneous in this study, there was no need for a detailed description of the radiation field. Instead, photon absorption rates were estimated from the incident irradiance as determined by actinometry.

A similar model was developed shortly after that by the group of Cassano [8,24] and applied to a variety of reactor geometries [25–27]. The advantage of this model is that it includes a detailed calculation of the radiation field, making it applicable to a much broader range of reactor geometries. However, the model was only tested under limiting conditions that greatly simplified the model. The model has not been tested outside the contaminant concentration range where first-order kinetics applies, and in all but one studies, the amount of UV irradiance was sufficiently low for the reaction rate to be first-order in UV irradiance. When the reaction rate is first-order in UV irradiance, the catalyst mass-weighted average photon absorption rate provides sufficient information to calculate exit pollutant concentrations, assuming plug flow conditions. Next, interactions with reaction products were not accounted for in this model; and the model assumes a mechanism based on OH radical attack, which is only realistic under humid conditions. Demeestere et al. [7] showed that some of the key parameters in the model depend on whether the process is

carried out under dry or moist conditions. Finally, the model of the Cassano group uses the concept of a constant primary quantum yield, which they defined as the fraction of electron–hole pairs that reach the catalyst surface without recombining, but this quantity can be expected to depend on light intensity.

Based on the agreement between the prediction of mathematical kinetic models and experimental data, hypotheses about the mechanism of the reaction can be tested, which lead to a better insight of the mechanism. There are two possible explanations of photocatalytic reactions. While some authors suggest an indirect oxidation via a surface bound hydroxyl radical [28,29], others propose a direct oxidation pathway via the valence-band hole [2,30–33]. The dominant mechanism will depend on the compound degraded. TCE is degraded photocatalytically in the absence of water vapor [7,34], indicating that direct oxidation is an important mechanism. An alternative that has been put forward is the oxidation of $O_2^{\bullet -}$ to two oxygen radicals by valence-band holes [35]. Chlorine radicals have been assumed to play a role as well, in a chain reaction [36,37].

The photocatalytic degradation of many types of VOCs proceeds through formation of intermediate products. According to the number of these intermediates, and the best suggested kinetic model, the mechanism can be proposed.

The aim of the present study is to assess the relevance of charge trapping in photocatalysis by kinetic modeling. The experimental data related to photocatalytic degradation of formate under continuous illumination in an aqueous system [38], was used for testing the UV irradiance dependency of the model. Once the relevance of charge trapping was established, we used the model to describe experimental data of Demeestere et al. [7] and determine charge trapping parameters. We also suggested a reaction mechanism for degradation of gaseous TCE on near-UV irradiated TiO_2 Degussa P25.

2. Model development

2.1. Kinetic model without considering charge trapping

The kinetic model developed by Demeestere et al. [7] for photocatalytic degradation of TCE, was simplified and applied to photocatalytic degradation of formate in aqueous phase. Simplification of the model was based on the assumption that formate adsorbed to the catalyst, F_{ads}, directly converts to CO_2. This happens through the following steps, which are summarized in Table 1.

The first step is linear formate adsorption–desorption equilibrium (Table 1, Eq. (5)) with K_F (l g^{-1}) the linear formate liquid–solid adsorption equilibrium constant. $[F]_{ads}$ (mmol g^{-1}) and $[F]_{aq}$ (mmol g^{-1}) are the concentration of formate in adsorbed and aqueous phases, respectively. Photoelectrochemical experiments of Villarreal et al. [39] have indicated that the adsorption of formate on TiO_2 is linear up to 10 mM, 100 times greater than the concentration in the experimental data used for the present study.

Production and recombination of electron–hole pairs $TiO_2(h^* + e^-)$ takes place via Eqs. (1) and (2) with r_{light} the electron–hole production rate (mmol g^{-1} s^{-1}) and r_{recomb} (mmol g^{-1} s^{-1}) and k_{recomb} (g $mmol^{-1}$ s^{-1}) the electron–hole recombination rate and rate constant, respectively. r_{light} is considered to be equal to the photon absorption rate per unit mass of catalyst, I (meinstein g^{-1} s^{-1}), multiplied by a primary quantum yield ϕ, defined by the fractions of absorbed photons that generate an electron–hole pair, irrespective of the fact if the electron–hole pair reaches the surface or not. In this paper we followed the implicit assumption of Cornu et al. [38] that $\phi = 1$. However, we included the parameter in case an independent determination becomes available. $[h^+] = [e^-]$ (mmol g^{-1}) represents the concentration of valence band (VB) holes and conduction band (CB) electrons, that can recombine (Eq. (2)) or initiate formate conversion directly or indirectly, e.g. via $^{\bullet}OH$, $Cl^{\bullet}$, $O^{\bullet -}$. Eq. (6) represents this conversion, in which r_F and k_F are the conversion rate and reaction rate constant of adsorbed formate, in (mmol g^{-1} s^{-1}) and (g $mmol^{-1}$ s^{-1}), respectively. The reason for equating $[h^+]$ and $[e^-]$ is the charge balance: inequality of $[h^+]$ and $[e^-]$ would charge the catalyst electrically. We assume that this does not happen to a significant extent. The reaction given in Eq. (6) is a simplification as other reaction products, like H_2O, are not considered.

Table 1
Reactions and rate equations

Reaction steps		Reaction rates
$TiO_2 + h\upsilon \rightarrow TiO_2(h^+ + e^-)$	(1)	r_{light}
$TiO_2(h^+ + e^-) \rightarrow TiO_2$	(2)	$r_{recomb} = k_{recomb}\,[h^+]^2$
$h^+ + trap \rightarrow h_{trap}$	(3)	$r_{trap} = k'_{trap}[trap][h^+]$
$h_{trap} \rightarrow trap$	(4)	$r_{reg} = k_{reg}\,[h_{trap}]$
$F_{aq} \rightleftarrows F_{ads}$ $\quad [F]_{ads} = K_F[F]_{aq}$	(5)	
$TiO_2(h^+) + F_{ads} \rightarrow TiO_2 + CO_2$	(6)	$r_F = k_F\,[h^+][F]_{ads}$
$TCE_g \rightleftarrows TCE_{ads}$ $\quad [TCE]_{ads} = K_{TCE}[TCE]_g$	(7)	
$P_g \rightarrow P_{ads}$	(8)	$r_{ads} = k_{ads}\,[P]_g$
$P_{ads} \rightarrow P_g$	(9)	$r_{des} = k_{des}\,[P]_{ads}$
$TiO_2(h^+) + TCE_{ads} \rightarrow TiO_2 + P_{ads}$	(10)	$r_{TCE} = k_{TCE}\,[h^+][TCE]_{ads}$
$nTiO_2(h^+) + P_{ads} \rightarrow TiO_2 + 2CO_2$	(11)	$r_P = k_p\,[h^+][P]_{ads}$
$TiO_2(h^+) + H_2O_{ads} \rightarrow TiO_2 + {}^{\bullet}OH + H^+$	(R1)	$r_{H_2O} = k_{H_2O}[h^+][H_2O]_{ads}$
$^{\bullet}OH + F_{ads} \rightarrow CO_2$	(R2)	$r_{OH,\,F} = k_{OH,\,F}\,[^{\bullet}OH][F]_{ads}$
$2\,^{\bullet}OH \rightarrow H_2O_2$	(R3)	$r_{OH,\,OH} = k_{OH,\,OH}\,[^{\bullet}OH]^2$
$^{\bullet}OH + TCE_{ads} \rightarrow P_{ads} + Cl^{\bullet}$	(R4)	$r_{In} = k_{In}[^{\bullet}OH]\,[TCE]_{ads}$
$Cl^{\bullet} + TCE_{ads} \rightarrow P_{ads} + Cl^{\bullet}$	(R5)	$r_{Pr} = k_{Pr}\,[Cl^{\bullet}]\,[TCE]_{ads}$
$2Cl^{\bullet} \rightarrow Cl_2$	(R6)	$r_{Te} = k_{Te}\,[Cl^{\bullet}]^2$

Considering steady-state concentrations of $[h^+]$ between t and $t + dt$, it can be assumed that

$$\frac{d[h^+]}{dt} = \phi I - k_F[h^+][F]_{ads} - k_{recomb}[h^+]^2 = 0 \tag{12}$$

$$\Rightarrow \quad [h^+] = \frac{-k_F[F]_{ads} + \sqrt{(k_F[F]_{ads})^2 + 4\phi I\, k_{recomb}}}{2\,k_{recomb}} \tag{13}$$

Substitution of Eq. (5) and (13) into Eq. (6) results into

$$r_F = \frac{(k_F K_F[F]_{aq})^2}{2\,k_{recomb}}\left(-1 + \sqrt{1 + \frac{4\phi I\, k_{recomb}}{(k_F K_F[F]_{aq})^2}}\right) \tag{14}$$

Apart from ϕ, this model has one adjustable parameter, $(k_F K_F)^2/k_{recomb}$. For consistency with the other models developed here, the value of $k_F K_F/\sqrt{k_{recomb}}$ will be reported. Eq. (14) is referred to as model F1 in the remainder of this paper.

2.2. Kinetic model with charge trapping

In this model, it is assumed that some of the holes get trapped according to Eq. (3), in which r_{trap} (mmol g^{-1} s^{-1}) and k_{trap} (g $mmol^{-1}$ s^{-1}) are the rate of the trapping reaction and its reaction rate constant, respectively.

In addition to Eq. (3), trap regeneration may occur. Eq. (4) describes this reaction, in which r_{reg} (mmol g^{-1} s^{-1}) and k_{reg} (s^{-1}) are the reaction rate of regeneration reaction and the reaction rate constant, respectively.

These assumptions lead to two different kinetic models, depending on the rate of Eq. (4). For heterogeneous photocatalysis on TiO_2, Ti(III)O–H^- and Ti(IV)O–H represent trap and h_{trap}, respectively [40].

2.2.1. Charge trapping with fast trap regeneration

In addition to Eqs. (5) and (6), Eq. (4) is also taken into account. Assuming a high reaction rate for the charge regeneration step

results in a constant concentration of trap, equal to the total trap concentration T.

As in Eq. (12), the steady state hypothesis for $[h^+]$ is applicable:

$$\Rightarrow \quad [h^+] = \frac{-(K_F k_F [F]_{aq} + k'_{trap} T) + \sqrt{(k_F K_F [F]_{aq} + k'_{trap} T)^2 + 4\phi I k_{recomb}}}{2 k_{recomb}} \tag{15}$$

Substitution of Eq. (5) and (15) into Eq. (6) results in:

$$r_F = \frac{k_F K_F [F]_{aq}}{2 k_{recomb}} (k_F K_F [F]_{aq} + k'_{trap} T) \left(-1 + \sqrt{1 + \frac{4 \phi I k_{recomb}}{(k_F K_F [F]_{aq} + k'_{trap} T)^2}} \right) \tag{16}$$

Apart from ϕ, this model has two adjustable parameters, $k_F K_F / \sqrt{k_{recomb}}$ and $k'_{trap} T / \sqrt{k_{recomb}}$. It is referred to as model F2 in the remainder of this paper.

Note that when $[F]_{aq}$ is small this equation is of the form $r_F = A[F]_{aq} (-1 + \sqrt{1 + BI})$, just like the model of Esterkin et al. [8] at constant humidity. Hence, the two models are mathematically equivalent at low pollutant concentration.

2.2.2. Charge trapping with slow trap regeneration

Considering both Eqs. (5) and (6) along with Eqs. (3) and (4), and assuming steady state for $[h^+]$, results in the nonlinear Eq. (17)

$$\frac{d[h^+]}{dt} = \phi I - \frac{K_F k_F [F]_l}{\sqrt{k_{recomb}}} (\sqrt{k_{recomb}} [h^+]) - (\sqrt{k_{recomb}} [h^+])^2 - \frac{(k'_{trap} T / \sqrt{k_{recomb}})(\sqrt{k_{recomb}} [h^+])}{1 + (k'_{trap} / \sqrt{k_{recomb}} k_{reg})(\sqrt{k_{recomb}} [h^+])} = 0 \tag{17}$$

$$T = [trap] + [h_{trap}] \tag{18}$$

In which T is a constant number, representing the total trap concentration (sum of Ti(III)O–H$^-$ and Ti(IV)O–H concentration) on the catalyst and has the unit of (mmol g^{-1}). Eq. (17) is solved for $\sqrt{k_{recomb}} [h^+]$. The reaction rate is calculated with Eq. (6) which is rewritten as:

$$r_F = \frac{k_F K_F [F]_{aq}}{\sqrt{k_{recomb}}} (\sqrt{k_{recomb}} [h^+]) \tag{19}$$

This model is referred to as model F3.

2.2.3. Effects of reactions with adsorbed water

A simplification of the models developed in the previous sections is that they do not consider the formation of $^\bullet$OH from adsorbed water and a hole. The $^\bullet$OH formed will also degrade formate efficiently, forming the $CO_2^{\bullet -}$ anion radical [41]. If the first step ($^\bullet$OH formation) is rate limiting, the kinetic equations will be very similar to the current model, and the effect of these parallel reactions can be absorbed by the kinetic parameters. Hence, the kinetic parameters should be considered as the parameters of a lumped model. A more complete model that incorporates $^\bullet$OH reactions explicitly will contain more adjustable parameters than can be justifiably estimated, but it is useful to derive such equations, and explore their properties. For convenience, the analysis is limited to extensions of model F1, but the approach can be applied to the other models as well.

The radical reactions relevant for the formate system are given in Table 1 as reactions (R1–R3). Applying the steady state approximation to $^\bullet$OH leads to:

$$[^\bullet OH] = \frac{-k_{OH,F} [F]_{ads} + \sqrt{(k_{OH,F} [F]_{ads})^2 + 4 k_{OH,OH} k_{H_2O} [H_2O]_{ads} [h^+]}}{2 k_{OH,OH}} \tag{20}$$

Since reaction with water provides an additional sink of electron–hole pairs, the steady-state equation for $[h^+]$ needs to be modified:

$$[h^+] = \frac{-k_F [F]_{ads} - k_{H_2O} [H_2O]_{ads} + \sqrt{(k_F [F]_{ads} + k_{H_2O} [H_2O]_{ads})^2 + 4\phi I k_{recomb}}}{2 k_{recomb}} \tag{21}$$

The overall reaction rate of formate is:

$$r_F = k_F [h^+] [F]_{ads} + k_{F,OH} [^\bullet OH] [F]_{ads} \tag{22}$$

with $[^\bullet OH]$ and $[h^+]$ given by Eqs. (20) and (21), respectively. This model is too complex to be fitted to the limited amount of data available. However, some special cases can be readily derived. For instance, when water is the main scavenger of holes, and the influence of formate on the build-up of electron–hole pairs is negligible, then Eq. (21) can be simplified as follows:

$$[h^+] = \frac{-k_{H_2O} [H_2O]_{ads} + \sqrt{(k_{H_2O} [H_2O]_{ads})^2 + 4\phi I k_{recomb}}}{2 k_{recomb}} \tag{23}$$

Hence, the reaction rate is given by the following equation:

$$r_F = \frac{k_F K_F k_{H_2O} [H_2O]_{ads}}{2 k_{recomb}} [F]_{aq} \left(-1 + \sqrt{1 + \frac{4\phi I k_{recomb}}{(k_{H_2O} [H_2O]_{ads})^2}} \right) + \frac{(k_{OH,F} K_F)^2}{2 k_{OH,OH}} [F]_{aq}^2 \left(-1 + \sqrt{1 + \frac{4 k_{OH,OH} (k_{H_2O} [H_2O]_{ads})^2}{2 k_{recomb} (k_{OH,F} K_F)^2 [F]_{aq}^2} \left(-1 + \sqrt{1 + \frac{4\phi I k_{recomb}}{(k_{H_2O} [H_2O]_{ads})^2}} \right)} \right) \tag{24}$$

Apart from ϕ, this equation has three adjustable parameters: $k_{OH,F}^2 K_F / k_{OH,OH}$, $k_{recomb} / (k_{H_2O} [H_2O]_{ads})^2$, and $k_F K_F k_{H_2O} [H_2O]_{ads} / k_{recomb}$. An extreme case of this model is when the reaction of holes with water is very fast, so $k_{recomb} / (k_{H_2O} [H_2O]_{ads})^2$ approaches zero because $(k_{H_2O} [H_2O]_{ads})^2$ becomes extremely large. In that case the square roots containing $k_{recomb} / (k_{H_2O} [H_2O]_{ads})^2$ approach 1, and the equation reduces to:

$$r_F = \frac{(k_{OH,F} K_F)^2}{2 k_{OH,OH}} [F]_{aq}^2 \left(-1 + \sqrt{1 + \frac{4 k_{OH,OH} \phi I}{(k_{OH,F} K_F)^2 [F]_{aq}^2}} \right) \tag{25}$$

This equation is of the same form as model F1.

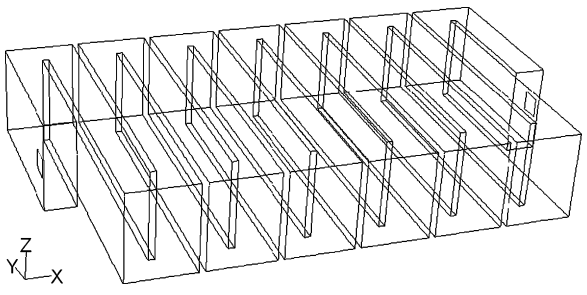

Fig. 1. Geometry of the photocatalytic reactor used by Demeestere et al. [7].

2.3. Kinetic model for photocatalytic degradation of gaseous TCE

The model for photocatalytic degradation of gaseous TCE will be tested with the experimental data of Demeestere et al. [7] in a serpentine flat-plate reactor with height 3 cm. The reactor is illustrated in Fig. 1. It is assumed that plug flow applies, and that there are no vertical (cross-sectional) concentration gradients. This might not be an intuitively obvious assumption for flow in a 3-cm channel at low Reynolds numbers. However, Martin et al. [42] found that the turns in a serpentine channel create a high degree of vertical mixing by vortices created by the turns, even under laminar conditions. Based on a classical Taylor–Aris analysis [16] applied to the residence time distribution determined by Demeestere et al. [7], the radial dispersion was estimated to be about 50 times the molecular diffusion, enough to limit vertical concentration variations to about 8%. Simulations with a two-dimensional model are under way. Preliminary research indicates that the kinetic parameter estimates are not very sensitive to the radial dispersion coefficient.

For the TCE degradation process, the same steps are followed as in [7]. In this set of reactions, first TCE adsorption on the catalyst takes place, according to Eq. (7) in Table 1. In this equation, K_{TCE} ($m^3\,g^{-1}$) is the linear TCE gas–solid adsorption equilibrium constant. The linearity of the TCE adsorption isotherm in the concentration range of 0.02–10.45 mg l^{-1} has been established by Demeestere et al. [43]. Adsorption and desorption of intermediate product P happen according to Eqs. (8) and (9) in which r_{ads} (mmol $g^{-1}\,s^{-1}$), k_{ads} ($m^3\,g^{-1}\,s^{-1}$), r_{des} (mmol $g^{-1}\,s^{-1}$) and k_{des} (s^{-1}) represent the P adsorption and desorption rates and rate constants, respectively. Electron–hole pairs are formed and recombined through Eqs. (1) and (2). Conversion of TCE and P occurs according to Eqs. (10) and (11) with r_{TCE} and r_P the degradation rates of TCE and P, respectively. k_{TCE} (g $mmol^{-1}\,s^{-1}$) and k_P (g $mmol^{-1}\,s^{-1}$) are TCE and P conversion rate constants, respectively. The first order behaviour of Eq. (11) in $[h^+]$ is based on the assumption that the conversion of P into CO_2 is the result of n consecutive reactions, with the first one being rate limiting. The reaction given in Eq. (11) is a simplified one as other reaction products, like H_2O, HCl, and Cl_2 are not considered.

In order to consider the effect of charge trapping, Eqs. (3) and (4) are used, along with the set of reactions describing photocatalytic degradation of TCE, suggested by Demeestere et al. [7]. Two models were developed, based on the assumption made for the rate of trap regeneration.

2.3.1. Charge trapping with fast trap regeneration

Reaction rates for TCE and intermediate product with consideration of charge trapping (i.e. adding Eq. (3)) are given in Eqs. (26) and (27) (see [7] for derivation of Eq. (26)).

$$r_{TCE} = [h^+]\sqrt{k_{recomb}}\,\frac{k_{TCE}K_{TCE}}{\sqrt{k_{recomb}}}[TCE]_g \tag{26}$$

$$r_p = \frac{k_P}{k_{des}\sqrt{k_{recomb}}} \times [h^+]\sqrt{k_{recomb}}\,\frac{k_{ads}[P]_g + (k_{TCE}K_{TCE}/\sqrt{k_{recomb}})[h^+]\sqrt{k_{recomb}}[TCE]_g}{1 + (k_P/k_{des}\sqrt{k_{recomb}})[h^+]\sqrt{k_{recomb}}} \tag{27}$$

in which $[h^+]\sqrt{k_{recomb}}$ is calculated from Eq. (28), which is derived from the steady state approximation for $[h^+]$ and $[P]_{ads}$.

$$\begin{aligned}
&([h^+]\sqrt{k_{recomb}})^3\left(-\frac{k_P}{k_{des}\sqrt{k_{recomb}}}\right)\\
&+([h^+]\sqrt{k_{recomb}})^2\left(-1-\frac{k_P}{k_{des}\sqrt{k_{recomb}}}\frac{k_{TCE}K_{TCE}}{\sqrt{k_{recomb}}}[TCE]_g-\frac{k_P}{k_{des}\sqrt{k_{recomb}}}\frac{k'_{trap}T}{\sqrt{k_{recomb}}}-n\frac{k_P}{k_{des}\sqrt{k_{recomb}}}\frac{k_{TCE}K_{TCE}}{\sqrt{k_{recomb}}}[TCE]_g\right)\\
&+([h^+]\sqrt{k_{recomb}})\left(I\frac{k_P}{k_{des}\sqrt{k_{recomb}}}-\frac{k_{TCE}K_{TCE}}{\sqrt{k_{recomb}}}[TCE]_g-\frac{k'_{trap}T}{\sqrt{k_{recomb}}}-n\frac{k_P}{k_{des}\sqrt{k_{recomb}}}k_{ads}\right)+I=0
\end{aligned} \tag{28}$$

This model is referred to as TCE2 (TCE1 being the original model of Demeestere et al. [7]).

2.3.2. Charge trapping with slow trap regeneration

Considering both Eqs. (3) and (4) next to Eq. (1), (2) and (7)–(11) gives, after rearrangement, the same equations as Eqs. (26) and (27) for reaction rates of TCE and intermediate product, respectively. In this case, $[h^+]\sqrt{k_{recomb}}$ is calculated from the fourth order polynomial Eq. (29).

$$\begin{aligned}
&([h^+]\sqrt{k_{recomb}})^4)\left(-\frac{k_P}{\sqrt{k_{recomb}}}\frac{k'_{trap}}{\sqrt{k_{recomb}}k_{reg}}\right)+([h^+]\sqrt{k_{recomb}})^3\\
&\times\left(-\frac{k_P}{\sqrt{k_{recomb}}}-k_{des}\frac{k'_{trap}}{\sqrt{k_{recomb}}k_{reg}}-\frac{k_{TCE}K_{TCE}}{\sqrt{k_{recomb}}}\frac{k_P}{\sqrt{k_{recomb}}}\frac{k'_{trap}}{\sqrt{k_{recomb}}k_{reg}}[TCE]_g-n\frac{k_P}{\sqrt{k_{recomb}}}\frac{k_{TCE}K_{TCE}}{\sqrt{k_{recomb}}}\frac{k'_{trap}}{\sqrt{k_{recomb}}k_{reg}}[TCE]_g\right)+([h^+]\sqrt{k_{recomb}})^2\\
&\times\left(-k_{des}-\frac{k_{TCE}K_{TCE}}{\sqrt{k_{recomb}}}\frac{k_P}{\sqrt{k_{recomb}}}[TCE]_g-n\frac{k_P}{\sqrt{k_{recomb}}}\frac{k_{TCE}K_{TCE}}{\sqrt{k_{recomb}}}[TCE]_g+\frac{k_P}{\sqrt{k_{recomb}}}\frac{k'_{trap}}{\sqrt{k_{recomb}}k_{reg}}I-\frac{k_{TCE}K_{TCE}}{\sqrt{k_{recomb}}}k_{des}\frac{k'_{trap}}{\sqrt{k_{recomb}}k_{reg}}[TCE]_g\right.\\
&\left.-n\frac{k_P}{\sqrt{k_{recomb}}}k_{ads}\frac{k'_{trap}}{\sqrt{k_{recomb}}k_{reg}}[p]_g-\frac{k_P}{\sqrt{k_{recomb}}}\frac{k'_{trap}T}{\sqrt{k_{recomb}}})+([h^+]\sqrt{k_{recomb}}\right)\\
&\times\left(\frac{k_P}{\sqrt{k_{recomb}}}I-\frac{k_{TCE}K_{TCE}}{\sqrt{k_{recomb}}}k_{des}[TCE]_g-n\frac{k_P}{\sqrt{k_{recomb}}}k_{ads}[p]_g+Ik_{des}\frac{k'_{trap}}{\sqrt{k_{recomb}}k_{reg}}-k_{des}\frac{k'_{trap}T}{\sqrt{k_{recomb}}}\right)+Ik_{des}=0
\end{aligned} \tag{29}$$

This model is referred to as TCE3.

2.3.3. Effects of $Cl^\bullet$ chain reactions

In order to account for chlorine radical chain reactions [44], the reactions (R1, R3–R6) were added to the mechanism. As with

formate, the full model contains too many adjustable parameters to be justifiably estimated, but inspection of the models provides some useful insights.

The steady state approximation applied to $Cl^{\bullet}$ leads to the following equation:

$$[Cl^{\bullet}] = \sqrt{\frac{k_{In}K_{TCE}[TCE]_g[^{\bullet}OH]}{2k_{Te}}} \quad (30)$$

In its general form, the steady state approximation applied to $^{\bullet}OH$ leads to the following equation:

$$[^{\bullet}OH] = \frac{k_{In}K_{TCE}[TCE]_g}{4k_{OH,OH}} \times \left(-1 + \sqrt{1 + \frac{8k_{OH,OH}k_{H_2O}[h^+][H_2O]_{ads}}{(k_{In}K_{TCE}[TCE]_g)^2}}\right) \quad (31)$$

Reaction (R4) leads to reaction products like CHClOHCCl(O) and CCl_2═CHOH [44], which are usually not observed. Hence, this reaction is only important as an initiator of the chlorine reaction chain and not as a pathway on its own. Given the high reactivity of $^{\bullet}OH$ for the carbon–carbon double bond, this is only possible if the $^{\bullet}OH$ concentration is very low, i.e. if reaction (R1) is very slow. In that case, Eq. (31) can be simplified to:

$$[^{\bullet}OH] = \frac{k_{H_2O}[h^+][H_2O]_{ads}}{k_{In}K_{TCE}[TCE]_g} \quad (32)$$

Hence, the chlorine radical concentration can be calculated as:

$$[Cl^{\bullet}] = \sqrt{\frac{k_{H_2O}[h^+][H_2O]_{ads}}{2k_{Te}}} \quad (33)$$

The overall reaction rate of TCE is (again discarding the direct contribution of (R4)):

$$r_{TCE} = k_{TCE}K_{TCE}[h^+][TCE]_g + k_{Pr}K_{TCE}\sqrt{\frac{k_{H_2O}[H_2O]_{ads}}{2k_{Te}}[h^+]}[TCE]_g \quad (34)$$

From the above equation and known properties of $[h^+]$ some features of the $Cl^{\bullet}$ chain reaction can be deduced. Analysis of Demeestere et al. [7] showed that the first term in Eq. (34) is proportional to I at low UV irradiance, and proportional to $I^{0.5}$ at high UV irradiance. The term is proportional to TCE concentration at low values, and independent of TCE concentration at high [TCE]. Hence, $[h^+]$ is proportional to I at low I and proportional to $I^{0.5}$ at high I, proportional to $[TCE]^0$ at low [TCE], and proportional to $[TCE]^{-1}$ at high [TCE]. From this it can be concluded that the second term in Eq. (34) is proportional to $I^{0.5}$ at low I and proportional to $I^{0.25}$ at high I; proportional to [TCE] at low [TCE], and proportional to $[TCE]^{0.5}$ at high [TCE]. These are unique features not encountered in other models. For instance, proportionality to I^n with $n < 0.5$ would normally be associated with mass transfer limitations. The chlorine radical chain reaction mechanism provides an alternative explanation for such kinetics.

3. Results and discussion

3.1. Formate degradation in aqueous solution

The quantum efficiency for the photocatalytic degradation of formate, Φ_F (dimensionless), was calculated in all cases as the degradation rate divided by the photon absorption rate:

$$\Phi_F = -\frac{r_F}{I} \quad (35)$$

The rate equation r_F was described by different kinetic models. Quantum efficiencies calculated based on a good kinetic model would be most consistent with experimental data. From experimental data for photocatalytic degradation of formate in an aqueous system under continuous illumination obtained by Cornu et al. [38], it was shown that by increasing the average photon absorption rate from 0.089 to 2.02 (μeinstein l^{-1} s^{-1}) the quantum efficiency is decreased from 0.074 to 0.021, respectively. Because the catalyst in the reactor is fluidized, changes of the illumination of individual particles are sufficiently fast to assume homogeneous continuous illumination of each catalyst particle. The photon absorption rates, as reported by Cornu et al. [38] in μeinstein l^{-1} s^{-1}, were converted to meinstein g^{-1} s^{-1} by dividing by the catalyst content in aqueous suspension (6 mg l^{-1}). By comparing these experimental values of quantum efficiency with model predictions, the photon absorption rate dependency of the kinetic model was tested.

As the error criterion, the sum of squares of quantum efficiency residuals
($SSQ = \sum(\text{residuals})^2 = \sum(\text{experimental data} - \text{model results})^2$)
is the objective function to be minimized for estimating model parameters. In accordance with the type of optimization problem, an appropriate method was applied for minimizing the objective function. For those cases in which $[h^+]$ was explicitly calculated, SSQ were minimized using the generalized reduced gradient (GRG2) algorithm for optimizing nonlinear parameter estimation problems, as implemented in the Microsoft Excel Solver software. For the case in which it is not possible to directly calculate $[h^+]$ (i.e. Model F3), trust-region reflective Newton was used as the algorithm of optimization function (lsqnonlin) in Matlab software.

Fig. 2 shows the data of Cornu et al. [38] together with fitted values of models F1, F2, and F3. It is clear from Fig. 2 that model F1 overestimates the UV irradiance dependence of the quantum efficiency. This is because model F1 does not incorporate charge trapping. Both last two models show excellent agreement with the data of Cornu et al. [38]. The parameter estimates are given in Table 2, together with the sum of squares of the residuals.

Comparing the curves in Fig. 2 and the SSQ values listed in Table 2, it is clear that both model F2 and model F3 including the effect of charge trapping, describe the experimental results more adequately than model F1 which is based on the kinetic model

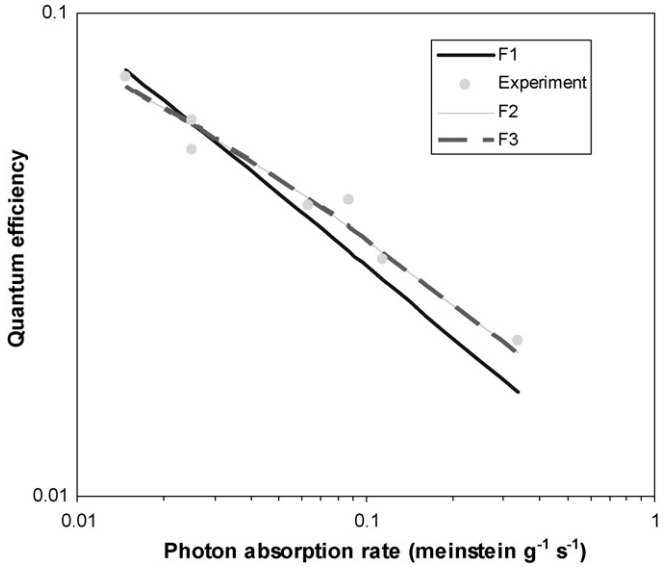

Fig. 2. Experimental (Cornu et al. [38]) and fitted (models F1, F2, and F3) quantum efficiency in the photocatalytic degradation of formate.

Table 2
Model parameters and sum of squares (SSQ) of model F1, F2, and F3 determined by least squares analysis. Optimization method: trust-region reflective Newton

Model parameter		F1	F2	F3
$\frac{k'_{trap}}{\sqrt{k_{recomb}}\,k_{reg}}$	$mmol^{-0.5}\ g^{0.5}\ s^{0.5}$	–	–	4.000×10^{-4}
$\frac{k_E K_E}{\sqrt{k_{recomb}}}$	$l\ mmol^{-0.5}\ g^{-0.5}\ s^{-0.5}$	9.642×10^{-2}	12.41×10^{-2}	12.41×10^{-2}
$\frac{k'_{trap}\,T}{\sqrt{k_{recomb}}}$	$mmol^{0.5}\ g^{-0.5}\ s^{-0.5}$	–	7.886×10^{-2}	7.888×10^{-2}
SSQ	–	16.95×10^{-5}	8.99×10^{-5}	8.99×10^{-5}

suggested by Demeestere et al. [7]. The accuracy of those models is confirmed in Table 2, showing smaller sums of squares of the residuals than what was obtained with model F1.

There is virtually no difference between the fitted data of model F2 and the fitted data of model F3. The parameters that both models have in common are also identical. This indicates that the difference between fast and slow charge trapping cannot be determined through observation of kinetic data. For reasons of simplicity it seems reasonable to assume fast charge trapping for the purpose of kinetic studies.

As an alternative, the effect of primary quantum yield was investigated as well. Using a value of $\phi = 0.136$ in model F1, it is possible to reproduce the accurate predictions of F2 and F3. However, this primary quantum yield is unrealistically low because the overall quantum efficiency sometimes reaches values of 0.3 and more [45,46]. Hence, it is concluded that charge trapping is required to explain the experimental data.

3.2. TCE degradation in the gas phase

For TCE as well as formate, modifications have been made to the model presented by Demeestere et al. [7]. In the present derivations of the model, the effect of charge trapping and regeneration has been taken into consideration.

The model parameters have been estimated to give the best fit to the experimental data obtained by Demeestere et al. [7]. Experiments were carried out in a flat-plate photoreactor at TCE inlet concentrations of 100–500 ppm, relative humidities (RH) of 0–62%, gas residence times of 2.5–60.3 s, and incident irradiance of 2.86×10^{-4} meinstein $g^{-1}\ s^{-1}$. Given the geometry of this reactor, the incident irradiance of the catalyst can be considered homogeneous across the entire reactor. This was confirmed with a simple radiation field model considering a line source of UV light and a cylindrical mirror. The incident irradiance showed a 6-cm plateau surrounded by a peak on each side at 4 cm from the centre, extending about 30% above the plateau. As the reactor was 10 cm wide, both peaks fell within the reactor, resulting in a coefficient of variance of 11.5%. The model predicts that the mirror increases average incident irradiance by 73%, close to the experimental value of 66% [47], confirming the reliability of the model. To estimate the error introduced by using average irradiance instead of the actual field, we compared average reaction rates in the actual field with reaction rates at average irradiance in the worst case scenario of reaction rates proportional to the square root of irradiance. The difference was 0.16%. Even for a particularly bad placement of the lamp with a peak irradiance of 3.6 times the average irradiance, the error was only 2.4%, clearly demonstrating that inhomogeneities in the radiation field are not as relevant for reactor performance as previously thought, as long as mass transfer limitations are not present.

Photon absorption rates were measured by actinometry, which actually measures incident radiation. However, photon absorption by TiO_2 in the near UV range is typically around 80% [48], and the reflected light was reflected back by a cylindrical aluminum surface behind the light source. To allow for the UV irradiation loss by reflection, we used 80% of the value of the incident radiation as determined by actinometry for I (photon absorption rate) in the calculation. The potential error in the parameter estimation from an incorrect estimate of I is discussed in Section 3.2.3.

3.2.1. Mechanistic considerations

The aim of this section is to reduce the number of adjustable parameters in the models by assigning a value to n in Eq. (11) based on an investigation of the reaction mechanism. One probable mechanism of conversion of TCE to products, takes place through three steps.

In the first step, TCE converts to dichloroacetyl chloride ($Cl_2CHCClO$). This was observed experimentally by some researchers [31,35,49,50]. They also proposed a mechanism to account for its formation. This mechanism requires one electron–hole pair.

In the second step dichloroacetyl chloride converts to phosgene (CCl_2O), CO_2 and Cl_2 with the aid of one electron–hole pair.

$$CHCl_2CClO + h^+ \rightarrow CHCl_2C^+ClO^\bullet$$

$$e^- + O_2 \rightarrow O_2^{\bullet -}$$

$$CHCl_2C^+ClO^\bullet + O_2^{\bullet -} \rightarrow CHCl_2CCl(O^\bullet)OO^\bullet$$

$$2CHCl_2CCl(O^\bullet)OO^\bullet \rightarrow 2CHCl_2CCl(O^\bullet)O^\bullet + O_2 \qquad \text{RussellMechanism}$$

$$CHCl_2CCl(O^\bullet)O^\bullet \rightarrow C^\bullet HCl_2 + CCl(O^\bullet)O$$

$$C^\bullet HCl_2 + O_2 \rightarrow C(OO^\bullet)HCl_2$$

$$2C(OO^\bullet)HCl_2 \rightarrow 2C(O^\bullet)HCl_2 + O_2 \qquad \text{RussellMechanism}$$

$$C(O^\bullet)HCl_2 \rightarrow COCl_2 + H^\bullet$$

$$CCl(O^\bullet)O \rightarrow CO_2 + Cl^\bullet$$

Several researchers proposed a mechanism mediated by OH radicals formed by holes attacking adsorbed water [35,50,51]. However, Demeestere et al. [7] and Amama et al. [44] found the highest photocatalytic degradation rate of TCE in the absence of water, indicating that there must be a mechanism similar to the above, not based on $^\bullet$OH attack, as well. Two mechanisms are responsible for the inhibitive effect of water: competitive adsorption of water and TCE on the catalyst surface [7], and inhibition of an oxidative chain reaction involving the chlorine radical [44].

In the third step, phosgene is converted to CO_2 and Cl_2, through reaction with one electron–hole pair. This was suggested by Joung et al. [35], as well.

Regarding the suggested mechanism, the number of intermediate products that use an electron–hole pair for reacting, (i.e. parameter of "n" in reaction rates) is equal to two. Considering this assumption it is reasonable to use a constant value of 2 for n. This value is considerably smaller than the one obtained by Demeestere et al. [7] based on purely kinetic considerations (n = 6–9). The reason for this difference is probably because charge trapping

Table 3
The results for the model regarding both assumptions of charge trapping and slow regeneration (model TCE3)

Group of parameters		RH < 0.8%	RH = 24.4 ± 1.7%	RH = 61.7 ± 3.3%
$\frac{k_P}{\sqrt{k_{recomb}}}$	$mmol^{-0.5}\ g^{0.5}\ s^{-0.5}$	2.751×10^{-1}	2.503×10^{-1}	2.383×10^{-1}
$\frac{k'_{trap}}{k_{reg}\sqrt{k_{recomb}}}$	$mmol^{-0.5}\ g^{0.5}\ s^{-0.5}$	6.684×10^{-7}	2.526×10^{-6}	1.227×10^{-6}
k_{ads}	$mmol^{0.5}\ g^{0.5}\ s^{0.5}$	8.509×10^{-7}	1.408×10^{-15}	1.36×10^{-13}
n	$m^3\ g^{-1}\ s^{-1}$	2	2	2
k_{des}	–	2.163×10^{-2}	1.294×10^{-2}	2.567×10^{-2}
$\frac{k_{TCE}K_{TCE}}{\sqrt{k_{recomb}}}$	s^{-1}	1.634×10^{-4}	6.426×10^{-3}	3.064×10^{-3}
$\frac{k'_{trap}T}{\sqrt{k_{recomb}}}$	$m^3\ mmol^{-0.5}\ g^{-0.5}\ s^{-0.5}$	2.618×10^{-1}	2.511×10^{-1}	2.708×10^{-1}
SSQ	$(mmol\ m^{-3})^2$	11.92	30.79	16.74

offers an alternative sink for electron–hole pairs that is not accounted for in the kinetic model of Demeestere et al. [7].

In moist air it is expected that OH radicals will play a role in the system, as Demeestere et al. [7] found two of the kinetic parameters to increase in humid air. Hydroxyl radicals are produced from the reaction of holes with adsorbed water [52], so again the mechanism can be considered as a hole-initiated system. The reaction of TCE with •OH leads to the production of monochloroacetyl chloride and a chlorine radical [51]. However, dichloroacetyl chloride (DCAC) is the dominant intermediate of the photocatalysis of TCE in both dry and humid conditions [49]. It seems likely that the chlorine radical chlorinates the monochloroacetyl chloride to DCAC under these conditions. The importance of the chlorine radical in secondary reactions in photocatalysis has been pointed out by Amama et al. [44] and Zhao et al. [53], who suggested a chain propagation mechanism. This mechanism was discussed in more detail in Section 2.3.3. One electron–hole pair has been used up at this point. Abstraction of H from DCAC by another OH radical could lead to phosgene in a reaction scheme very similar to the one above. Abstraction of chlorine from phosgene by •OH would complete the reaction scheme with three OH radicals, each resulting from a hole. It is concluded that $n = 2$ is plausible under humid conditions, where •OH mediated reactions occur, as well.

3.2.2. Kinetic results

The results for the model considering charge trapping and slow regeneration (model TCE3) are presented in Table 3. For comparison, the sums of squares of the residuals obtained with the original model of Demeestere et al. [7] are 9.93, 30.95, and 16.46 at relative humidities of RH ≤0.8%, 24.4 ± 1.7%, and 61.7 ± 3.3%, respectively. The values are very similar, although our value of SSQ is slightly larger than the value of Demeestere et al. [7] at RH < 0.8%.

In fitting the parameters, it was interestingly observed that parameter $k'_{trap}/\sqrt{k_{recomb}}\,k_{reg}$, which describes the rate of trap regeneration relative to the other key processes, does not have any influence on the value of other parameters and the model fit. The same observation was made with the formate data (see above). The ineffectiveness of this parameter implies the fact that the charge regeneration reaction is not relevant for the reaction kinetics, and can be considered fast for the purpose of simplicity. So it can be assumed that

$$[h_{trap}] = 0, \quad \text{and} \quad [\text{trap}] = T$$

By substitution and rearrangement, we get the same equations as model TCE2 (Eqs. (26) and (27) for reaction rate and Eq. (28) for calculating $[h^+]\sqrt{k_{recomb}}$).

With the assumption of fast regeneration, and fixing n to the reasonable value of two, values of the other parameters and SSQ are calculated and presented in Table 4.

As can be noted, comparably good results are obtained. In addition, by assuming fast regeneration, unnecessary complication of the reactions is avoided.

3.2.3. Comparison with formate degradation kinetics

The value of $k'_{trap}T/\sqrt{k_{recomb}}$ found based on formate data (Table 2) is about a factor 10–20 lower than the value based on TCE data (Table 4). However, this parameter describes processes occurring in the catalyst, independent of the chemical that is being degraded. Consequently, one could expect that this parameter should be the same in both systems. It was observed that the values of the parameters $k_P/k_{des}\sqrt{k_{recomb}}$, $k_{TCE}K_{TCE}/\sqrt{k_{recomb}}$ and $k'_{trap}T/\sqrt{k_{recomb}}$ are highly correlated and only their ratios can be estimated accurately. For that reason we repeated the parameter estimation with the value of $k'_{trap}T/\sqrt{k_{recomb}}$ fixed at $0.0789\ mmol^{0.5}\ g^{-0.5}\ s^{-0.5}$, the value obtained with model F2 based on the kinetic data of Cornu et al. [38]. The results are shown in Table 5 for model TCE2. The quality of the fit decreased only slightly (at most 1.01%) by fixing the value of $k'_{trap}T/\sqrt{k_{recomb}}$, indicating that this is acceptable as a provisional value for this parameter pending more data that will allow for an unambiguous

Table 4
The results of the kinetic model with only consideration of charge trapping in the reaction (model TCE2)

Group of parameters		RH < 0.8%	RH = 24.4 ± 1.7%	RH = 61.7 ± 3.3%
$\frac{k_P}{k_{des}\sqrt{k_{recomb}}}$	$mmol^{-0.5}\ g^{0.5}\ s^{0.5}$	$4.138 \times 10^{+3}$	$8.195 \times 10^{+3}$	$6.835 \times 10^{+3}$
k_{ads}	$m^3\ g^{-1}\ s^{-1}$	8.496×10^{-7}	2.22×10^{-20}	2.22×10^{-20}
n	–	2	2	
$\frac{k_{TCE}K_{TCE}}{\sqrt{k_{recomb}}}$	$m^3\ mmol^{-0.5}\ g^{-0.5}\ s^{-0.5}$	5.317×10^{-2}	2.315×10^{-2}	2.339×10^{-2}
$\frac{k'_{trap}T}{\sqrt{k_{recomb}}}$	$mmol^{0.5}\ g^{-0.5}\ s^{-0.5}$	8.534×10^{-1}	9.064×10^{-1}	1.795
SSQ	$(mmol\ m^{-3})^2$	11.91	30.78	16.52

Table 5
The results of the kinetic model with only consideration of charge trapping in the reaction; fixed value of $k'_{trap}T/\sqrt{k_{recomb}}$ (model TCE2)

Group of parameters		RH < 0.8%	RH = 24.4 ± 1.7%	RH = 61.7 ± 3.3%
$\frac{k_P}{k_{des}\sqrt{k_{recomb}}}$	$mmol^{-0.5}\ g^{0.5}\ s^{0.5}$	3.890 × 102	7.296 × 102	3.084 × 102
k_{ads}	$m^3\ g^{-1}\ s^{-1}$	8.629×10^{-7}	2.22×10^{-20}	2.22×10^{-20}
n	–	2	2	2
$\frac{k_{TCE}K_{TCE}}{\sqrt{k_{recomb}}}$	$m^3\ mmol^{-0.5}\ g^{-0.5}\ s^{-0.5}$	5.030×10^{-3}	2.066×10^{-3}	1.058×10^{-3}
$\frac{k'_{trap}T}{\sqrt{k_{recomb}}}$	$mmol^{0.5}\ g^{-0.5}\ s^{-0.5}$	0.0789	0.0789	0.0789
SSQ	$(mmol\ m^{-3})^2$	12.04	30.83	16.57

estimate of this parameter. Based on the experience with formate in Section 3.1, the light intensity dependence may well be the key here. In the mean time the parameter values in Table 5 should be considered as relative values. It is concluded that the TCE data and the formate data are consistent with each other with respect to charge trapping.

As indicated earlier, the measured value of I might be too high because actinometry actually measures incident radiation. For that reason, the parameters were estimated with a photon absorption rate of 0.8 times the incident radiation (Tables 3–5). However, it can be assumed that the overestimate is less than 20% due to back-reflection. For sensitivity analysis, the parameters were estimated with photon absorption rates of 0.7 and 0.9 times the incident radiation as well. The effect on the parameter estimate is about 10–20%. This is the potential error of the parameter estimates due to the uncertainty of the photon absorption rate. For higher relative humidities the potential error is even less, 0–15%. The value of the sum of squares of the residuals (in $mmol^2\ m^{-6}$) is changing by about ±11%, ±1% and ±1% for <0.8%, 24.4%, and 61.7 % RH, respectively. It is concluded that an improved estimation of I is useful, but not crucial for the use of this model.

3.2.4. Discussion of parameter values

The values of $k_{TCE}K_{TCE}/\sqrt{k_{recomb}}$ for TCE degradation are consistently about a factor 6 larger than the results found by Demeestere et al. [7]. The consistency is not surprising as the models are strongly related, and the parameter estimates are based on the same data set. Given the fact that the new parameter set gives relative provisional values at this point, the factor 6 difference is not an indication of inconsistency. The values of K_{TCE} were investigated by Demeestere et al. [43]. At dry conditions a value of $0.403 \times 10^{-3}\ m^3\ g^{-1}$ was found for TCE on TiO_2. At relative humidities above 20%, K_{TCE} decreased exponentially with RH, with calculated values of $0.0491 \times 10^{-3}\ m^3\ g^{-1}$ and $0.0259 \times 10^{-3}\ m^3\ g^{-1}$ for 24.4% and 61.7% RH, respectively. This leads to estimates for $k_{TCE}/\sqrt{k_{recomb}}$ of 12.481, 42.077 and 40.849 $mmol^{-0.5}\ g^{0.5}\ s^{-0.5}$ for 0.8%, 24.4%, and 61.7% RH, respectively. This confirms the finding of Demeestere et al. [7], who concluded that the presence of an adsorbed water layer hinders the adsorption of TCE molecules on the surface, but stimulates degradation once the molecules are adsorbed. They attributed the effect to •OH radical formation from adsorbed water.

The value of k_{ads} is of the same order of magnitude as the value of Demeestere et al. [7] at 0.8% RH, and essentially zero at higher moisture content. This means that water adsorbed on the catalyst surface forms an effective barrier to reaction products in the gas phase.

The value of $k_P/k_{des}\sqrt{k_{recomb}}$ goes through a maximum versus relative humidity. This can be explained as a combined effect of two factors. First, $k_P/\sqrt{k_{recomb}}$ can be expected to show an increase between 0.8% and 24.4% RH, and to stay constant at higher relative humidities. k_{des}, on the other hand, can be expected to increase continuously. The combined effect is a maximum value at intermediate relative humidities.

Based on quality of fit with experimental data, there is no significant difference between the model presented here and the original model of Demeestere [7]. However, the new model has two major advantages. The first is the fact that the new model works quite well with a value of parameter n equal to 2. As discussed above, this value is more realistic than the fitted value of Demeestere et al. [7], so it can be expected that the new model represents fundamental processes on the catalyst better than the original model. A second advantage is the more realistic description of irradiance dependence, as discussed in Section 3.1. It is expected that the model will allow for more accurate irradiance dependence calculations than the original model. More experimental research is necessary to confirm this, and will enable a more definitive determination of the parameter $k'_{trap}T/\sqrt{k_{recomb}}$.

4. Conclusion

The model of Demeestere et al. [7] for photocatalytic kinetics was extended to include charge trapping. Based on literature data of formate photocatalysis in aqueous phase, it was shown that considering charge trapping improved the kinetic model, as supported by a halving of sum of squares of the residuals. It resulted in a better prediction of the relation between photon absorption rate and quantum yield. This is an indication that charge trapping influences the UV irradiance dependency of photocatalytic degradation rates.

Consideration of charge trapping in the case of gaseous TCE photocatalytic degradation leads to a more realistic estimate of the number of reaction steps in comparison with the previous model presented by Demeestere et al. [7]. Although all the charge trapping models applied fitted the data well, the fast trap regeneration model assuming two intermediate products seems to be more appropriate as it is consistent with the number of electron–hole pairs expected to be consumed in the process given the mechanism. The slow trap regeneration model, which also has this feature, is more complex than warranted by the data. The parameter estimates are only meaningful as relative values due to their strong correlation. However, based on all the model fits a common parameter, $k'_{trap}T/\sqrt{k_{recomb}}$, has been tentatively assigned a value of 0.0789 $mmol^{0.5}\ g^{-0.5}\ s^{-0.5}$. More research in a wider range of concentrations and UV light irradiance is needed for a better evaluation of this parameter.

Acknowledgement

The Natural Sciences and Engineering Research Council (NSERC) of Canada and the Canada Research Chairs program are acknowledged for financial support.

References

[1] A. Bouzaza, A. Laplanche, J. Photochem. Photobiol. A Chem. 150 (2002) 207–212.
[2] J. Peral, X. Domenech, D.F. Ollis, J. Chem. Technol. Biotechnol. 70 (1997) 117–140.
[3] J. Wan-Kuen, K.H. Park, Chemosphere 57 (2004) 555–565.
[4] J. Zhao, X.D. Yang, Building Environ. 38 (2003) 645–654.
[5] Y.D. Hou, W.C. Wang, L. Wu, Z.X. Ding, X.Z. Fu, Environ. Sci. Technol. 40 (2006) 5799–5803.
[6] F.B. Li, X.Z. Li, C.H. Ao, M.F. Hou, S.C. Lee, Appl. Catal. B Environ. 54 (2004) 275–283.
[7] K. Demeestere, A. De Visscher, J. Dewulf, M. Van Leeuwen, H. Van Langenhove, Appl. Catal. B Environ. 54 (2004) 261–274.
[8] C.R. Esterkin, A.C. Negro, O.M. Alfano, A.E. Cassano, AIChE J. 51 (2005) 2298–2310.
[9] M.R. Hoffmann, S.T. Martin, W.Y. Choi, D.W. Bahnemann, Chem. Rev. 95 (1995) 69–96.
[10] K.H. Wang, Y.H. Hsieh, C.H. Lin, C.Y. Chang, Chemosphere 39 (1999) 1371–1384.
[11] S.E. Braslavsky, Pure Appl. Chem. 79 (2007) 293–465.
[12] W.A. Jacoby, D.M. Blake, R.D. Noble, C.A. Koval, J. Catal. 157 (1995) 87–96.
[13] K.H. Wang, H.H. Tsai, Y.H. Hsieh, Appl. Catal. B Environ. 17 (1998) 313–320.
[14] J.M. Herrmann, Top. Catal. 34 (2005) 49–65.
[15] A. Bouzaza, C. Vallet, A. Laplanche, J. Photochem. Photobiol. A Chem. 177 (2006) 212–217.
[16] H.S. Fogler, Elements of Chemical Reaction Engineering, Prentice Hall International Series, 1999.
[17] H. Ibrahim, H. de Lasa, AIChE J. 50 (2004) 1017–1027.
[18] S.B. Kim, S.C. Hong, Appl. Catal. B Environ. 35 (2002) 305–315.
[19] C.M. Ma, Y. Ku, React. Kinet. Catal. Lett. 89 (2006) 293–301.
[20] S. Yamazaki, S. Tanaka, H. Tsukamoto, J. Photochem. Photobiol. A Chem. 121 (1999) 55–61.
[21] I. Salvado-Estivill, D.M. Hargreaves, G.L. Puma, Environ. Sci. Technol. 41 (2007) 2028–2035.
[22] W. Wang, L.W. Chiang, Y. Ku, J. Hazard. Mater. 101 (2003) 133–146.
[23] T.N. Obee, R.T. Brown, Environ. Sci. Technol. 29 (1995) 1223–1231.
[24] G.E. Imoberdorf, H.A. Irazoqui, A.E. Cassano, O.M. Alfano, Ind. Eng. Chem. Res. 44 (2005) 6075–6085.
[25] G.E. Imoberdorf, A.E. Cassano, O.M. Alfano, H.A. Irazoqui, AIChE J. 52 (2006) 1814–1823.
[26] G.E. Imoberdorf, A.E. Cassano, H.A. Irazoqui, O.M. Alfano, Chem. Eng. Sci. 62 (2007) 1138–1154.
[27] G.E. Imoberdorf, H.A. Irazoqui, O.M. Alfano, A.E. Cassano, Chem. Eng. Sci. 62 (2007) 793–804.
[28] G. Mills, M.R. Hoffmann, Environ. Sci. Technol. 27 (1993) 1681–1689.
[29] C.S. Turchi, D.F. Ollis, J. Catal. 122 (1990) 178–192.
[30] R.B. Draper, M.A. Fox, Langmuir 6 (1990) 1396–1402.
[31] M. Hegedus, A. Dombi, Appl. Catal. A Gen. 271 (2004) 177–184.
[32] I.K. Konstantinou, T.A. Albanis, Appl. Catal. B Environ. 49 (2004) 1–14.
[33] M. Hegedus, A. Dombi, Appl. Catal. B Environ. 53 (2004) 141–151.
[34] H. Liu, S.A. Cheng, J.Q. Zhang, C.N. Cao, W.C. Jiang, Chemosphere 35 (1997) 2881–2889.
[35] S.K. Joung, T. Amemiya, M. Murabayashi, K. Itoh, Chem. A Eur. J. 12 (2006) 5526–5534.
[36] C.H. Hung, B.J. Marinas, Environ. Sci. Technol. 31 (1997) 562–568.
[37] M. Mohseni, Chemosphere 59 (2005) 335–342.
[38] C.J.G. Cornu, A.J. Colussi, M.R. Hoffmann, J. Phys. Chem. B. 105 (2001) 1351–1354.
[39] T.L. Villarreal, R. Gomez, M. Neumann-Spallart, N. Alonso-Vante, P. Salvador, J. Phys. Chem. B. 108 (2004) 15172–15181.
[40] S.H. Szczepankiewicz, J.A. Moss, M.R. Hoffmann, J. Phys. Chem. B. 106 (2002) 2922–2927.
[41] N.A. Aristova, N.K. Vel Leitner, I.M. Piskarev, High Energy Chem. 36 (2002) 197–202.
[42] J. Martin, P. Oshkai, N. Djilali, J. Fuel Cell Sci. Technol. 2 (2005) 70–80.
[43] K. Demeestere, J. Dewulf, H. Van Langenhove, B. Sercu, Chem. Eng. Sci. 58 (2003) 2255–2267.
[44] P.B. Amama, K. Itoh, M. Murabayashi, J. Mol. Catal. A Chem. 176 (2001) 165–172.
[45] H. Ibrahim, H. de Lasa, Chem. Eng. Sci. 58 (2003) 943–949.
[46] T. Torimoto, Y. Aburakawa, Y. Kawahara, S. Ikeda, B. Ohtani, Chem. Phys. Lett. 392 (2004) 220–224.
[47] M. Van Leeuwen, Verwijdering van gehalogeneerde en aromatische verbindingen uit afvalgas via TiO_2-gekatalyseerde foto-oxidatie, M.Sc. Thesis, Ghent University, Belgium, 2003.
[48] C.R. Esterkin, A.C. Negro, O.M. Alfano, A.E. Cassano, AIChE J. 48 (2002) 832–845.
[49] P.B. Amama, K. Itoh, M. Murabayashi, J. Mol. Catal. A Chem. 217 (2004) 109–115.
[50] S. Rodrigues, K.T. Ranjit, S. Uma, I.N. Martyanov, K.J. Klabunde, J. Catal. 230 (2005) 158–165.
[51] S. Yamazakinishida, S. Cerveramarch, K.J. Nagano, M.A. Anderson, K. Hori, J. Phys. Chem. 99 (1995) 15814–15821.
[52] J.F. Fan, J.T. Yates, J. Am. Chem. Soc. 118 (1996) 4686–4692.
[53] L.H. Zhao, S. Ozaki, M. Itoh, M. Murabayashi, Electrochemistry 70 (2002) 8–12.